J. Appl. Comput. Mech., 7(2) (2021) 520-527
DOI: 10.22055/JACM.2020.35381.2646

ISSN: 2383-4536
jacm.scu.ac.ir

Shahid Chamran University of Ahvaz

Journal of Applied and Computational Mechanics

Research Paper

Heat Transport Exploration of Free Convection Flow inside Enclosure Having Vertical Wavy Walls

Md. Fayz-Al-Asad[1], Md. Nur Alam[2], Cemil Tunç[3], M.M.A. Sarker[1,4]

[1] Department of Civil Engineering, Dhaka International University, Dhaka-1212, Bangladesh

[2] Department of Mathematics, Pabna University of Science and Technology, Pabna- 6600, Bangladesh

[3] Department of Mathematics, Faculty of Sciences, Van Yuzuncu Yil University, 65080, Van, Turkey

[4] Department of Mathematics, Bangladesh University of Engineering and Technology, Dhaka-1000, Bangladesh

Received October 11 2020; Revised November 05 2020; Accepted for publication November 10 2020.
Corresponding author: Cemil Tunç (tunccemil@gmail.com)

Abstract. This paper expresses a numerical study of flow features and heat transport inside enclosure. Governing equations will be discretized by finite-element process with a collected variable arrangement. The assumptions of the Grashof number (10^3 - 10^6), aspect ratio (1.0 – 2.0), wave ratio (0.0 - 0.40) concerning a fluid with Pr = 0.71. Streamlines and isotherm lines are utilized to show the corresponding flow and thermal field inside a cavity. Global and local distributions Nusselt numbers are displayed for the before configuration. Finally, velocity and temperature profiles are displayed for some selected positions inside an enclosure for a better perception of the flow and thermal field.

Keywords: Free convection, Aspect ratio, Wave ratio, Finite element method, Wavy wall.

1. Introduction

Over the years, numerous pioneers have been tremendous progress in the subject of irregular shape enclosure. Several kinds of geometries, models, and types of fluid analyzed in the recent year include wavy [1-3], triangular [4, 5], hexagonal [6], rectangular [7, 8], square [9, 10], and, etc. Natural convection [11-21] and free convection [22-26] inside enclosures has been explored widely for various boundary conditions, Hartmann numbers, Rayleigh numbers, nano-fluids, aspect ratios, steady and unsteady case. Adding a wavy wall cavity has a notable impact on both flow phenomena, heat transfer and numerous studies have reviewed heat transfer properties following the before-mentioned requirements. It is worth mentioning that the present work simulation was finite element method, but the Ref. [22] was a simulation finite volume method. Geometry and boundary condition's mathematical expressions section is looking same, but the main differences between our paper and that in the [22] are given as: In Ref. [22], two straight walls are adiabatic and the right wavy wall is heated temperature and the left wavy wall is cold temperature. In spite of these case, in our paper, one straight wall is heated temperature and another one is a cold temperature, and both wavy walls are cold temperature. Öztop et al. [27] considered on magneto hydrodynamic combined convection in a nanofluid filled and heated bottom wavy walled enclosure. They decided that the gradient temperature was reduced by raising nano-particles in volume fraction. Ghahremani [28] explored natural convection in an enclosure with variable thermal expansion coefficient and nanoparticles. Alsabery et al. [29, 30] studied the effect on a rotating cylinder in an enclosure with an entropy analysis and vertical wavy wall. Menni et. al. [31] examined fluid dynamics and heat transfer in a rectangular duck with staggered baffles. Siddiqui et al. [32] scrutinized combined convective flow in moving wall enclosure through a micropolar fluid. Bilal et al. [33] analyzed Finite element strategy visualization regarding heat transfer report of a triangular cavity involving a square cylinder. Menni et. al. [34] investigated fluid flow and heat shift across staggered '+' shaped obstacles. In the prospect of this evidence, the existing research can be implemented in numerous applied mathematics, mathematical physics and engineering such as nuclear power plants, solar cells, heat exchanging devices, and so on. Sheikholeslami et al. [35] investigated the swirl generator, and a four-lobed pipe was employed regarding nanofluid. Sheikholeslami [36] studied nanofluid MHD flow inside a porous cavity applying Darcy laws. Sheikholeslami [37] also determined exergy and entropy analysis of nanofluid under Lorentz force's impact through a porous media. Bakheet Almatrafi et al. [38], Nur Alam and Tunç [39, 40] investigated the construction of soliton solutions and found exact solutions of certain partially differential equations and give some interesting applications about the considered equations.

In the existing inquiry, heat transport exploration of free convection flow inside enclosure having a vertical wavy wall. Based on the above-mentioned literature survey, there are numerous inquiries concerning free convection flow inside the enclosure having wavy sidewalls that are not yet tackled by researchers.

Published online: November 21 2020

2. Mathematical modeling

Analyzing two-dimensional convection in the enclosure with a vertical wavy sidewall as presented in Figure 1.

The flow in the geometry-shape is examined steady, laminar, and Boussinesq approximations are valid. The governing non-linear dimensionless equations are the continuity, Navier-Stokes, and the energy balance equation of the incompressible viscous flow are

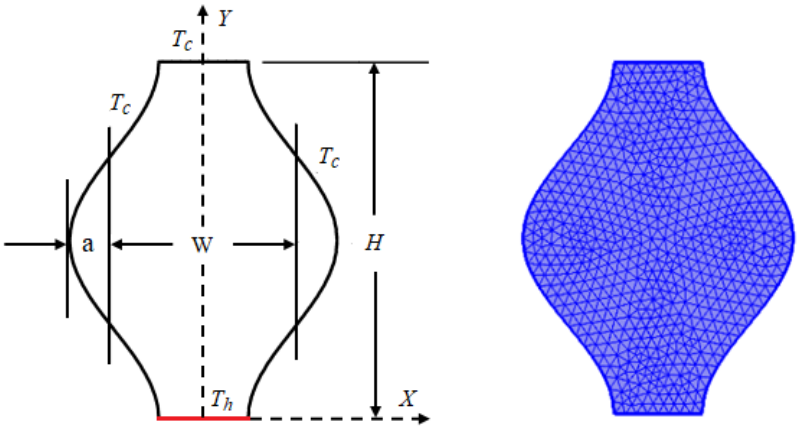

Fig. 1. Schematic design of a vertical wavy cavity.

$$\frac{\partial U}{\partial X}+\frac{\partial U}{\partial Y}=0 \tag{1}$$

$$U\frac{\partial U}{\partial X}+V\frac{\partial U}{\partial Y}=-\frac{\partial P}{\partial X}+\frac{1}{\sqrt{Gr}}\nabla^2 U \tag{2}$$

$$U\frac{\partial V}{\partial X}+V\frac{\partial V}{\partial Y}=-\frac{\partial P}{\partial Y}+\frac{1}{\sqrt{Gr}}\nabla^2 V+\theta \tag{3}$$

$$U\frac{\partial \theta}{\partial X}+V\frac{\partial \theta}{\partial Y}=\frac{1}{\Pr\sqrt{Gr}}\nabla^2\theta \tag{4}$$

The above equations (1)-(4) have been dimensionless forms by estimating varying lengths with average diameter W, *velocity components* with a reference velocity ($V_0=\sqrt{g\beta\Delta TW}$), pressure ($\rho V_0^2$), non-dimensional temperature $\theta=(T-T_\infty)/\Delta T$; where $\Delta T=T_h-T_c$.

Boundary conditions:

Figure 1 exposes the geometry-shape is considered the present inquiry with various boundary conditions and the axis system. The vertical wavy walls and shape of a wave surface are represented as equations (5a) and (5b). Boundary conditions (dimensionless form) for the consideration problem are noted as:

$$U=0,V=0,\theta=0,X=\left(\frac{1}{2}-\lambda\right)+\lambda\left[1-\sin\frac{\pi}{2}\left(1+\frac{4Y}{A}\right)\right] \quad \text{for} \quad 0\le Y\le A \tag{5a}$$

$$U=0,V=0,\theta=0,X=-\left(\frac{1}{2}-\lambda\right)-\lambda\left[1-\sin\frac{\pi}{2}\left(1+\frac{4Y}{A}\right)\right] \quad \text{for} \quad 0\le Y\le A \tag{5b}$$

$$U=0,V=0,\theta=0,-\left(\frac{1}{2}-\lambda\right)\le X\le\left(\frac{1}{2}-\lambda\right) \quad \text{for} \quad Y=A \tag{5c}$$

$$U=0,V=0,\theta=1,\ -\left(\frac{1}{2}-\lambda\right)\le X\le\left(\frac{1}{2}-\lambda\right) \quad \text{for} \quad Y=0 \tag{5d}$$

Local and global Nusselt numbers on the hot wall which is determined by Selimefendigil *et al.* [12] and Mahmud *et al.* [22]

$$Nu_L=\frac{h_L W}{k} \quad \text{and} \quad Nu_{av}=\frac{1}{H}\int_0^H Nu_L dX \tag{6}$$

3. Solution methodology

The governing dimensionless equations (1) - (4) together with the non-dimensional boundary conditions (5a)-(5d) are solved numerically using Galerkin weighted residual (GWR) finite element approach.

Firstly, we apply a penalty finite element technique (FET) by eliminating the pressure via a penalty parameter (γ) and the incompressibility criteria given by equation (1) as follows:

$$P=-\gamma\left(\frac{\partial U}{\partial X}+\frac{\partial V}{\partial Y}\right) \tag{7}$$

Manipulating Eq. (7), the momentum Eqs. (2) - (3) decrease to

$$U\frac{\partial U}{\partial X}+V\frac{\partial U}{\partial Y}=\gamma\left(\frac{\partial U}{\partial X}+\frac{\partial V}{\partial Y}\right)+\frac{1}{\sqrt{Gr}}\nabla^2U \tag{8}$$

$$U\frac{\partial V}{\partial X}+V\frac{\partial V}{\partial Y}=\gamma\left(\frac{\partial U}{\partial X}+\frac{\partial V}{\partial Y}\right)+\frac{1}{\sqrt{Gr}}\nabla^2V+\theta \tag{9}$$

Secondly, the system of the momentum and energy equations (8), (9), and (4) respectively with boundary conditions (5a) - (5d) is determined by using Galerkin finite element process [41, 42]. The interpolation function approximating the velocity segments (U and V), and temperature distribution (ϑ) applying the basic set $\{\Phi_j\}_{j=1}^{k}$ as

$$U\approx\sum_{j=1}^{k}U_j\Phi_j(X,Y),\quad V\approx\sum_{j=1}^{k}V_j\Phi_j(X,Y)\ \text{and}\ \ \theta\approx\sum_{j=1}^{k}\theta_j\Phi_j(X,Y) \tag{10}$$

The non-linear residual equations (8), (9), and (4) are obtained from Galerkin weighted residual through finite element approach at nodes of the internal domain (Ω):

$$\begin{aligned}R_i^{(1)}\approx{}&\sum_{j=1}^{k}U_j\int_{\Omega}\left[\left(\sum_{j=1}^{k}U_j\Phi_j\right)\frac{\partial\Phi_j}{\partial X}+\left(\sum_{j=1}^{k}V_j\Phi_j\right)\frac{\partial\Phi_j}{\partial Y}\right]\Phi_i\,dXdY+\gamma\left[\sum_{j=1}^{k}U_j\int_{\Omega}\frac{\partial\Phi_i}{\partial X}\frac{\partial\Phi_j}{\partial X}dXdY+\sum_{j=1}^{k}V_j\int_{\Omega}\frac{\partial\Phi_i}{\partial X}\frac{\partial\Phi_j}{\partial Y}dXdY\right]\\&+\frac{1}{\sqrt{Gr}}\sum_{j=1}^{k}U_j\int_{\Omega}\left[\frac{\partial\Phi_i}{\partial X}\frac{\partial\Phi_j}{\partial X}+\frac{\partial\Phi_i}{\partial Y}\frac{\partial\Phi_j}{\partial Y}\right]dXdY\end{aligned} \tag{11}$$

$$\begin{aligned}R_i^{(2)}\approx{}&\sum_{j=1}^{k}V_j\int_{\Omega}\left[\left(\sum_{j=1}^{N}U_j\Phi_j\right)\frac{\partial\Phi_j}{\partial X}+\left(\sum_{j=1}^{k}V_j\Phi_j\right)\frac{\partial\Phi_j}{\partial Y}\right]\Phi_i\,dXdY+\gamma\left[\sum_{j=1}^{k}U_j\int_{\Omega}\frac{\partial\Phi_i}{\partial Y}\frac{\partial\Phi_j}{\partial X}dXdY+\sum_{j=1}^{k}V_j\int_{\Omega}\frac{\partial\Phi_i}{\partial Y}\frac{\partial\Phi_j}{\partial Y}dXdY\right]\\&+\frac{1}{\sqrt{Gr}}\sum_{j=1}^{k}U_j\int_{\Omega}\left[\frac{\partial\Phi_i}{\partial X}\frac{\partial\Phi_j}{\partial X}+\frac{\partial\Phi_i}{\partial Y}\frac{\partial\Phi_j}{\partial Y}\right]dXdY+\int_{\Omega}\left(\sum_{j=1}^{k}\theta_j\Phi_j\right)\Phi_i\,dXdY\end{aligned} \tag{12}$$

$$R_i^{(3)}\approx\sum_{j=1}^{k}\theta_j\int_{\Omega}\left[\left(\sum_{j=1}^{k}U_j\Phi_j\right)\frac{\partial\Phi_j}{\partial X}+\left(\sum_{j=1}^{k}V_j\Phi_j\right)\frac{\partial\Phi_j}{\partial Y}\right]\Phi_i\,dXdY+\frac{1}{Pr\sqrt{Gr}}\sum_{j=1}^{k}\theta_j\int_{\Omega}\left[\frac{\partial\Phi_i}{\partial X}\frac{\partial\Phi_j}{\partial X}+\frac{\partial\Phi_i}{\partial Y}\frac{\partial\Phi_j}{\partial Y}\right]dXdY \tag{13}$$

where i, j and k are the residual, nodes, and iteration number respectively. Then the next steps the above integral equations (11) - (13) were performed by Gaussian quadrature method.

Finally, the Newton-Raphson iteration procedure was applied to iteratively solve the residual equations. The details solution may be found in earlier works [19, 21, and 32]. A convergence of a computational procedure is achieved once the following convergence criteria or condition are satisfied as

$$\left|\frac{\Gamma^{m+1}-\Gamma^{m}}{\Gamma^{m+1}}\right|\le10^{-5} \tag{14}$$

4. Grid test and accuracy

4.1 Grid Test

In the present inquiry, a nonuniform, free triangular and non-staggered grid system is employed. Five discrete grid systems of finite element are used to analyze the significance of grid size on the exactness of the predicted outcomes. The numerical results are displayed in Table 1 and as viewed in Figure 2; show insignificant changes toward the G4 grid and beyond. Hence, the G4 grid provided a satisfactory solution for all computations of this investigation.

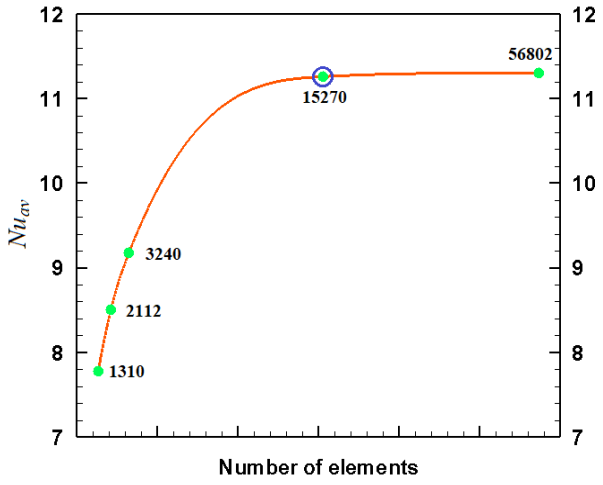

Fig. 2. Grid testing for Nu_{av} for several elements

Table 1. Grid testing for Nu_{av} at various grid sizes for $\lambda = 0.25$, $A = 2$ and $Ra = 10^5$.

Grid size	Nodes	Element	Nu_{av}
G1	698	1310	7.7776
G2	1109	2112	8.5024
G3	1688	3240	9.1816
G4	**7779**	**15270**	**11.263**
G5	28678	56802	11.305

4.2 Grid Test

Validation of the present numerical code is performed by comparing the current work with the published work of Jani *et al.* [23], as represented in Figure 3. The confidence in verifying the present results is applied to provide the accuracy of the current numerical code.

5. Discussion on results

The manuscript should be prepared using the present template. The present computational study focuses on the range of the following parameter: Grashof number (10^3 - 10^6), aspect ratio (1 - 2), wave ratio (0.0 - 0.40) for a fluid with Prandtl number is 0.71.

Stream functions and isotherm lines

Stream and isotherm lines for various parameters with a uniform heating bottom and cold from additional walls depict in Figure 4 - 5 for λ = 0.25 - 0.30, A = 2.0 at four distinct Grashof numbers. Hot fluid flows up on the heating wall and shifts to the cold walls and then mixes with fluid that moves upward on the upper wall. Figure 4 - 5 exposes that stream functions (ψ), a couple of elliptic-shaped eddies are produced in the lower half inside enclosure for λ = 0.25 - 0.30, A = 2.0. Due to a Grashof numbers increase, the flow construction becomes stronger, besides the rotating eddies ascend the top wall. Conduction heat transport is viewed form the isotherm lines (T) is also depicted in these Figure 4 - 5 for λ = 0.25 - 0.30, A = 2.0. Conduction is minor dominant at this Grashof number $Gr = 10^3$ and 10^4. Also accretive to Grashof number ($Gr = 10^6$), the isotherm lines are dominant close to the wavy wall, which means enhancing heat transport through convection. The structure of a thermal frame can be watched from isotherm lines at $Gr = 10^5$ and 10^6.

Flow and Temperature profiles

Velocity component (V) temperature profiles (ϑ) are exhibited in Figure 6 (a) and (b) for $A = 2.0$ (aspect ratio), λ = 0.25 (surface waviness) and four distinct Grashof number (Gr) at $Y = 1.0$. At $Gr = 10^3$ velocity profile is similar to the horizontal midline of the enclosure. The velocity profile is a minor change for $Gr = 10^4$ than for $Gr = 10^3$. A further accretion in Gr raises the peak velocities, but now the velocity profiles move towards the vertical and the top walls. According to Figure 6 (b) illustrates the $Gr = 10^3$ and $Gr = 10^4$ temperature distribution is a trivial variation. Moreover, Gr increases the peak temperature, but now the temperature profiles move towards the upper wall.

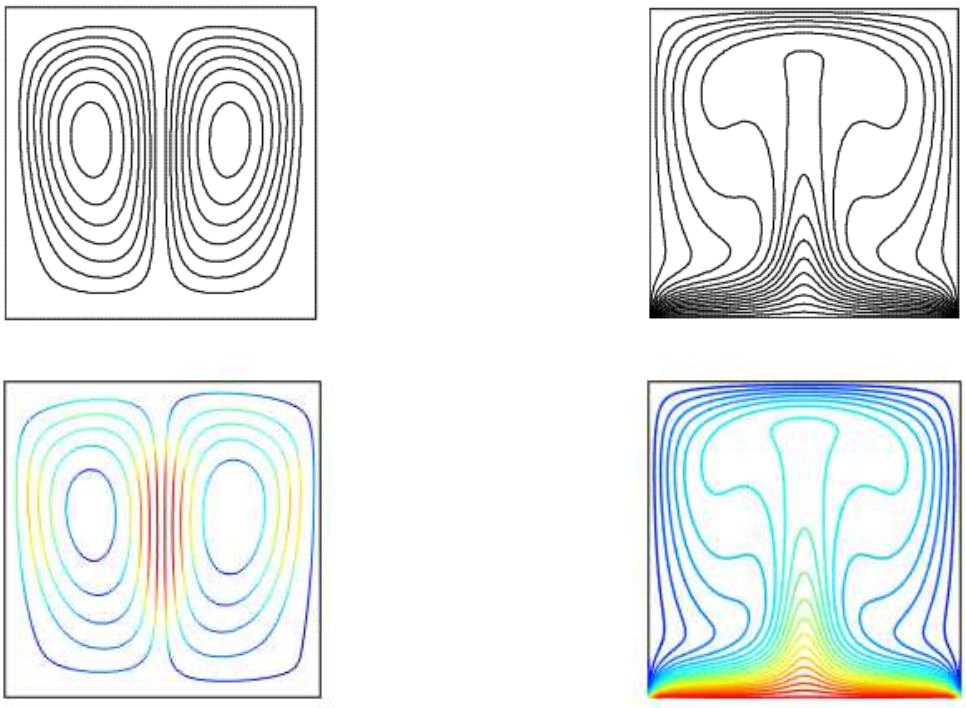

Fig. 3. Jani *et al.* [23] upper row and the present study bottom row, streamlines (left) and isotherms (right) for $Ha = 0$, $Gr = 10^5$ and $Pr = 0.71$.

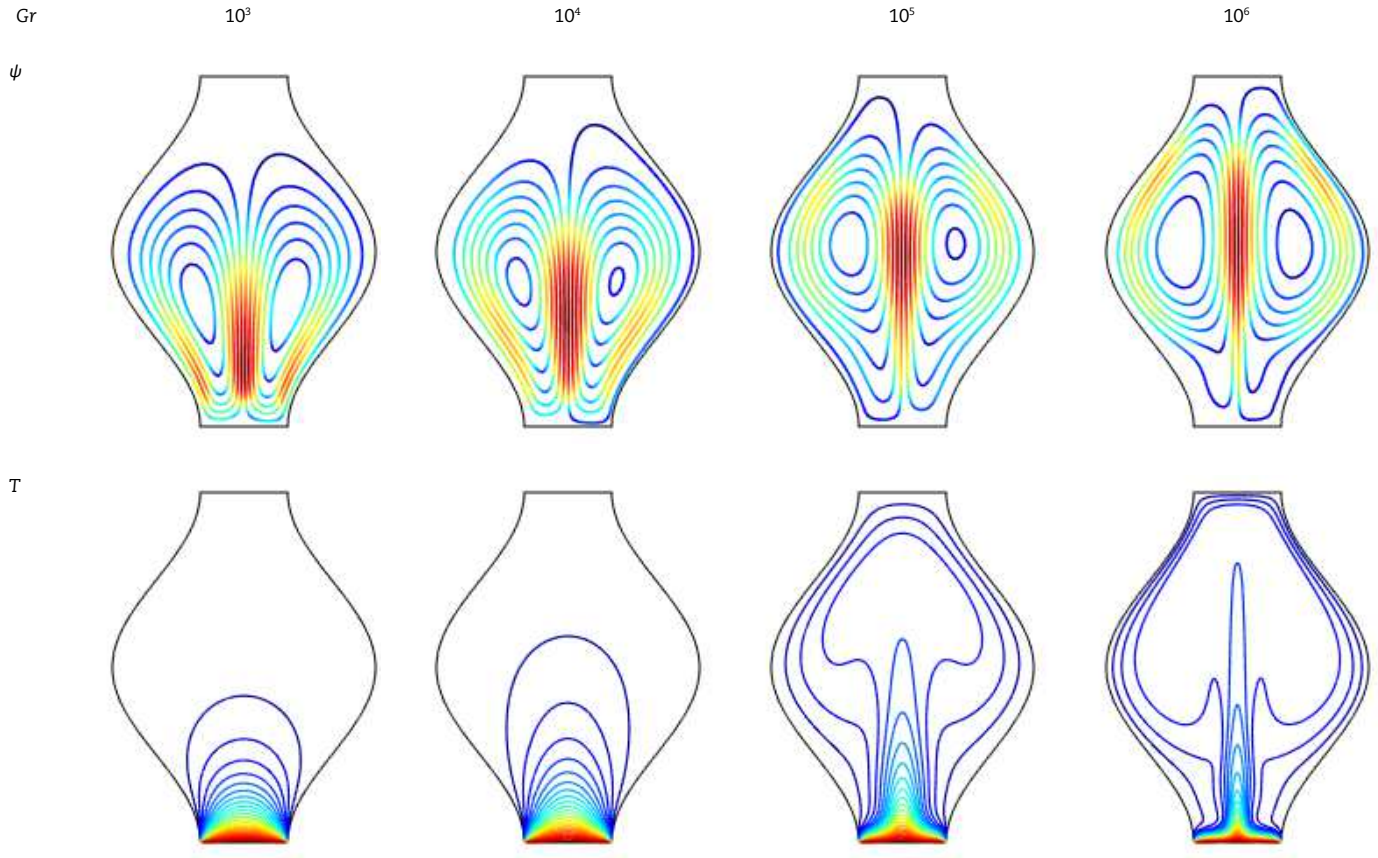

Fig. 4. Stream and isotherm lines for various Gr at $\lambda = 0.25$ and $A = 2.0$.

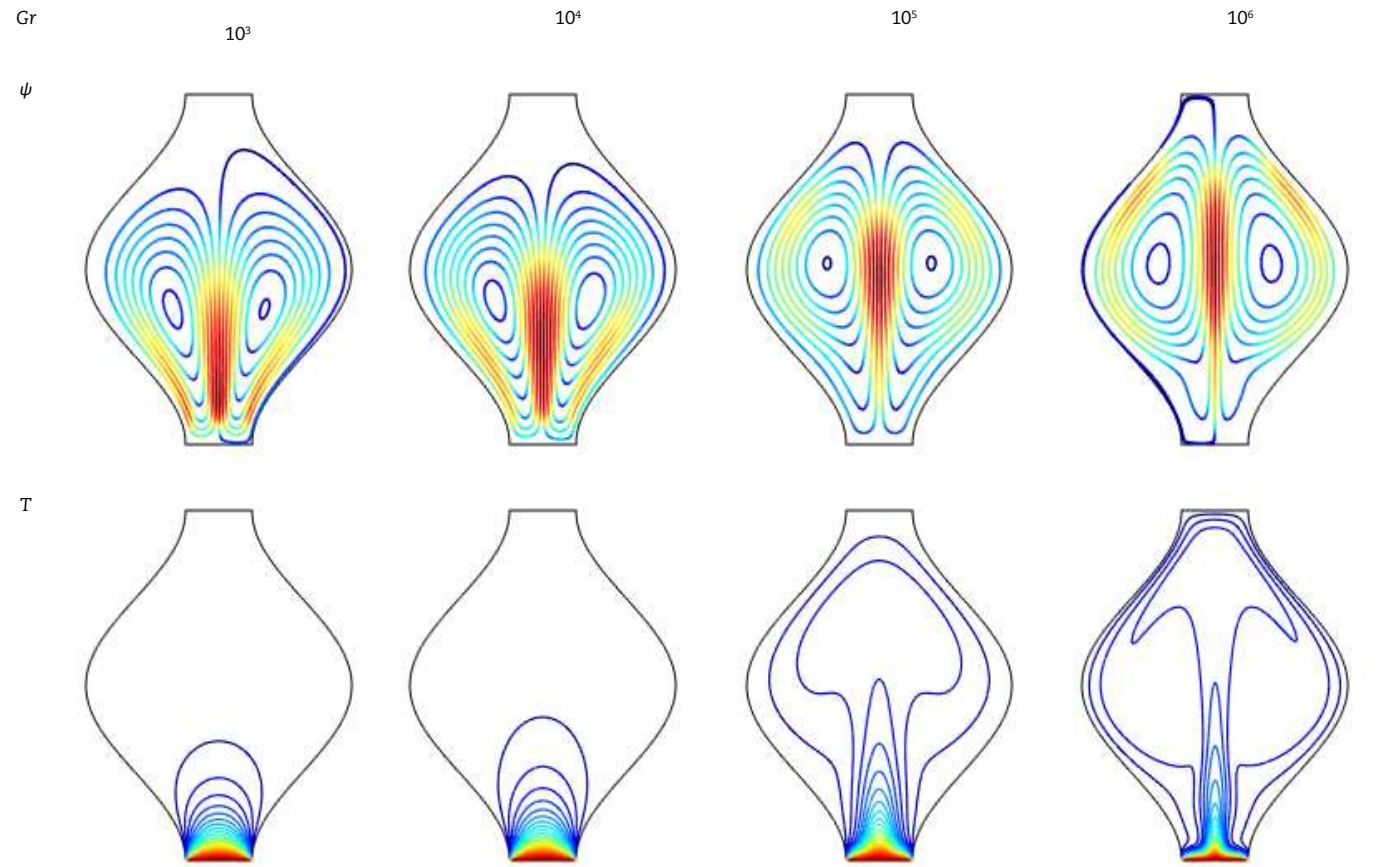

Fig. 5. Stream and isotherm lines for various Gr at $\lambda = 0.30$ and $A = 2.0$.

Nusselt number distribution

Figure 7 (a) and (b) reveal the impact of *Gr*, λ, and *A* = 2.0 at the heating bottom wall. Figure 7 (a) distribution of a local Nusselt number on the heating wall for selected Grashof number (*Gr*). For the place of great values Gr, the thermal layout is very high-pitched in wavy walls. Also noticed the middle of the hot wall, the Nusselt number equals zero, and change insignificant with a raise in Grashof number. Figure 7 (b) arrangement of mean Nusselt number on the hot wall for chosen surface waviness (λ), the thermal performance is enhanced significantly than the level wall.

Variation of aspect ratio and surface waviness

Figure 8(a) exposes the variation of mean Nusselt number for a heating wall for three separate aspect ratios *A* = 1.0, 1.50, 2.0, Grashof number (*Gr* = 10^3, 10^4, 10^5, 10^6) at fixed surface waviness λ = 0.25. As the aspect ratio grows, the mean Nusselt number slowly progresses each Grashof number, and in this management gradient temperature rate is significantly dominated by convection. Figure 8(b) bare the waviness (λ) for *A* = 2.0 and *Gr* = 10^5 along the heating wall. As surface waviness rises, the gradient temperature extends the convective heat-releasing boosts.

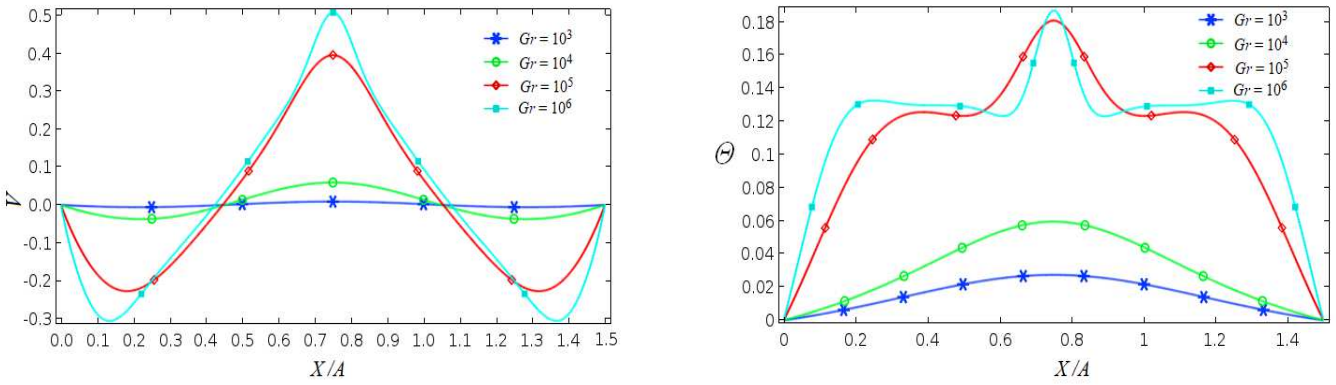

(a) (b)

Fig. 6. (a) Velocity and (b) Temperature field for λ = 0.25 and *A* = 2.0.

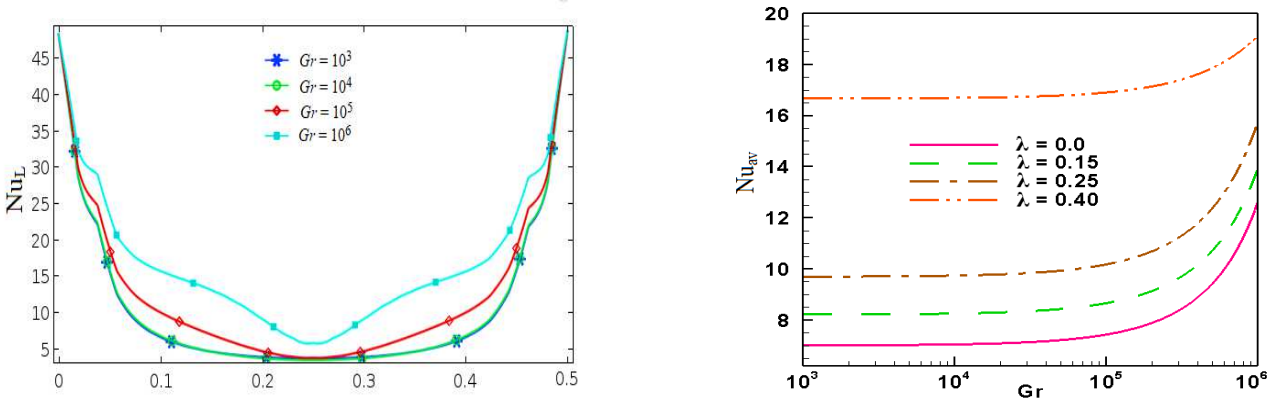

(a) (b)

Fig. 7. (a) Nu_L and (b) Nu_{av} for *A* = 2.0.

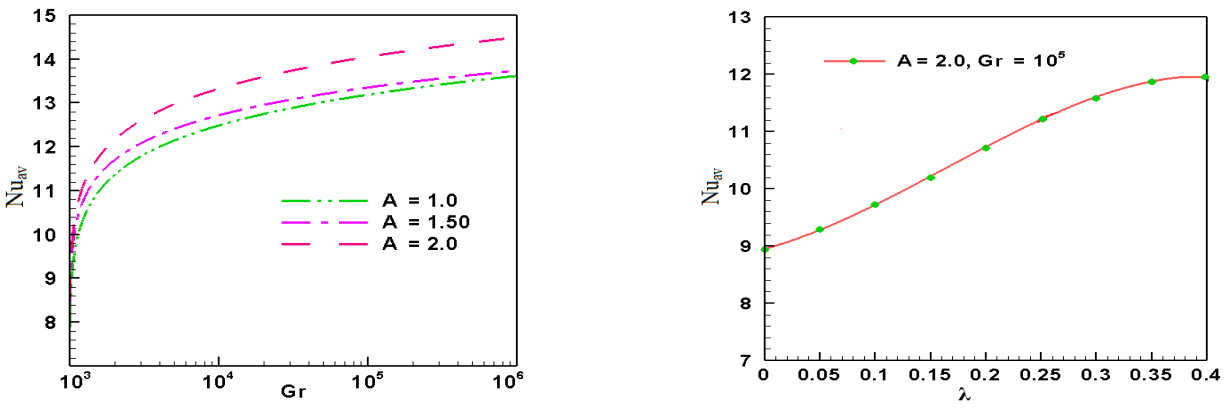

(a) (b)

Fig. 8. (a) Aspect ratio for λ = 0.25 and (b) Surface waviness for *A* = 2.0

6. Conclusion

The principal objective of the present analysis is to examine the impacts of Grashof number, aspect ratio, waviness on the thermal variation, and flow stream of free convection inside a wavy compartment covered with Newtonian fluid. The numerical code is confirmed associating by the published studies. Our predictions explain that the heat-releasing depends strongly on aspect ratio and surface waviness. For a distinct aspect ratio, heat removal is low variety and independent of a Grashof number. The high surface waviness, the heat transport is enhanced. For a fixed aspect ratio, Grashof number heat removal boosts steadily with a raises of surface waviness ascends 0.40, over which heat discharge grows again.

Author Contributions

Md. Fayz-Al-Asad planned the scheme, initiated the project, and suggested the experiments; Md. Nur Alam conducted the experiments and analyzed the empirical results; C. Tunç developed the mathematical modeling and examined the theory validation. The manuscript was written through the contribution of all authors. All authors discussed the results, reviewed, and approved the final version of the manuscript.

Conflict of Interest

The authors declared no potential conflicts of interest with respect to the research, authorship, and publication of this article.

Funding

The authors received no financial support for the research, authorship, and publication of this article.

Nomenclature

a	Amplitude of the wave
A	Aspect ratio, H / W
g	Gravitational force, m.s^{-2}
Gr	Grashof number, $g\beta\Delta TW^3/\upsilon^2$
h	Heat transfer coefficient, W. m^{-2}. K^{-1}
H	Height of the cavity, m
k	Thermal conductivity, W. m^{-1}. K^{-1}
Nu_L	Local Nusselt number
Nu_{av}	Average Nusselt number
P	Dimensionless pressure
Pr	Prandlt number, ν / α
U, V	Dimensionless velocity in X and Y direction respectively
W	Average width of the cavity

Greek symbols

α	Thermal diffusivity, m^2.s^{-1}
β	Thermal expansion coefficient, K^{-1}
λ	Surface waviness, a / W
ρ	Density of the fluid, kg.m^{-3}
υ	Kinematic viscosity, m^2.s^{-1}
ϑ	Dimensionless temperature

Subscripts

c	Cooled
h	Heated

References

[1] Alsabery, A. I., Ghalambaz, M., Armaghani, T., Chamkha, A. J., Hashim, I., Pour, M. S., Role of rotating cylinder toward mixed convection inside a wavy heated cavity via two-phase, *Nanomaterials*, 10, 2020, 1138.
[2] Azizul, F. M., Alsabery, A. I., Hashim, I., Chamkha, A. J., Heatlines visualisation of mixed convection double lid-driven cavity having heated wavy wall, *Journal of Thermal Analysis and Calorimetry*, 2020, DOI: 10.1007/s10973-020-09806-5.
[3] Azizul, F. M., Alsabery, A. I., Hashim, Heatlines visualisation of mixed convection flow in a wavy heated cavity filled with nanofluids and having inner solid block, *International Journal of Mechanical Science*, 175, 2020, 105529.
[4] Islam, T., Parveen, N., Asad, M. F. A., Hydromagnetic natural convection heat transfer of copper-water nanofluid within a right-angled triangular cavity, *International Journal of Thermofluid Science and Technology*, 7(3), 2020, 070304.
[5] Haq, R. U., Soomro, F. A., Öztop, H. F., Mekkaoui, T., Thermal management of water-based carbon nanotubes enclosed in a partially heated triangular cavity with heated cylindrical obstacle, *International Journal of Heat and Mass Transfer*, 131, 2019, 724-736.
[6] Asad, M. F. A., Sarker, M. M. A., Munshi, M. J. H., Numerical investigation of natural convection flow in a hexagonal enclosure having vertical fin, *Journal of Scientific Research*, 11(2), 2019, 173-183.
[7] Gangawane, K. M., Gupta, S., Mixed convection characteristics in rectangular enclosure containing heated elliptical block: effect of direction of moving wall, *International Journal of Thermal Science*, 130, 2019, 397–406.
[8] Louaraychi, A., Lamsaadi, M., Namimi, M., Harf, H. E., Kaddiri, M., Raji, A., Hasnaoui, M., Mixed convection heat transfer correlations in shallow rectangular cavities with single and double-lid driven boundaries, *International Journal of Heat and Mass Transfer*, 132, 2019, 394-406.
[9] Chen, H., Lin, M., Chang, J., Numerical and experimental studies of natural convection in a heated cavity with a horizontal fin on a hot side wall, *International Journal of Heat and Mass Transfer*, 124, 2018, 1217-1229.
[10] Asad, M. F. A., Sarker, M. M. A., Hossain, M. A., Numerical investigation of MHD mixed convection heat transfer having vertical fin in a lid-driven square cavity, *AIP Conference Proceding*, 2121, 2019, 030023-6.
[11] Basak, T., Chamakha, A. J., Heatline analysis on natural convection for nanofluids confined within square cavities with various thermal boundary conditions, *International Journal of Heat and Mass Transfer*, 55, 2012, 5526-5543.
[12] Selimefendigil, F., Öztop, H. F., Al-Salem, K., Natural convection of ferrofluids in partially heated square enclosures, *Journal of Magnetism and Magnetic Materials*, 372, 2014, 122-133.
[13] Dalal, A., Das, M. K., Natural convection in a cavity with wavy wall heated from below and uniformly cooled from the top and both sides, *Journal of Heat Transfer*, 128 (7), 2006, 717-725.
[14] Boulahia, Z., Wakif, A., Sehaqui, R., Numerical modeling of natural convection heat transfer in a wavy wall enclosure filled by a Cu-water nanofluid with a square cooler, *Journal of Nanofluids*, 6(2), 2017, 1-10.
[15] Uddin, K. M. S., Saha, L. K., Numerical solution of 2-D incompressible driven cavity flow with wavy bottom surface, *American Journal of Applied Mathematics*, 3(1-1), 2015, 30-42.
[16] Javaherdeh, K., Moslemi, M., Shahbazi, M., Natural convection of nanofluid in a wavy cavity in the presence of magnetic field on variable heat surface temperature, *Journal of Mechanical Science and Technology*, 31, 2017, 1937-1945.
[17] Ashorynejad, H. R., Shahriari, A., MHD natural convection of hybrid nanofluid in an open wavy cavity, *Results in Physics*, 9, 2018, 440-455.
[18] Asad, M. F. A., Munshi, M. J. H., Sarker, M. M. A., Effect of fin length and location on natural convection heat transfer in a wavy cavity, *International Journal of Thermofluid Science and Technology*, 7(3), 2020, 070303.
[19] Basak, Roy, T., S., Bal akrishnan, A. R., Effects of thermal boundary conditions on natural convection flows within a square cavity, *International Journal of Heat and Mass Transfer*, 49(23-24), 2006, 4525-4535.

[20] Rostami, J., Unsteady natural convection in an enclosure with vertical wavy walls, *Heat and Mass Transfer*, 44, 2008, 1079–1087.
[21] Basak, T., Roy, S., Role of 'Bejan's heatlines' in heat flow visualization and optimal thermal mixing for differentially heated square enclosures, *International Journal of Heat and Mass Transfer*, 51(13-14), 2008, 3486-3503.
[22] Mahmud, S., Das, P. K., Hyder, N., Islam, A.K.M. S., Free convection in an enclosure with vertical wavy walls, *International Journal of Thermal Science*, 41(5), 2002, 440–446.
[23] Jani, S., Mahmoodi, M., Amini, M., Magnetohydrodynamic free convection in a square cavity heated from below and cooled from other walls, *International Journal of Mechanical, Aerospace, Industrial and Mechatronics Engineering*, 7(4), 2013, 331-336.
[24] Grosan, T., Revnic, C., Pop, I., Ingham, D. B., Free convection heat transfer in a square cavity with a porous medium saturated by a nanofluid, *International Journal of Heat and Mass Transfer*, 87, 2015, 36-41.
[25] Sheremet, M., Cimpean, D., Pop, I., Free convection in a partially heated wavy porous cavity filled with a nanofluid under the effects of Brownian diffusion and thermophoresis, *Applied Thermal Engineering*, 113, 2017, 413–418.
[26] Munshi, M. J. H., Asad, M. F. A., Bhowmik, R. K., Sarker, M. M. A., MHD free convection heat transfer having vertical fin in a square wavy cavity, *International Journal of Statistics Applied Mathematics*, 4(3), 2019, 32-38.
[27] Öztop, H. F., Sakhrieh, A., Nada, E. A., Al-Salem, K., Mixed convection of MHD flow in nanofluid filled and partially heated wavy walled lid-driven enclosure, *International Communications in Heat and Mass Transfer*, 86, 2017, 42-51.
[28] Ghahremani E., Transient natural convection in an enclosure with variable thermal expansion coefficient and nanoparticles, *Journal of Applied and Computational Mechanics*, 4(3), 2018, 133-139.
[29] Alsabery, A. I., Ismael, M. A., Chamakha, A. J., Hashim, I., Numerical investigation of mixed convection and entropy generation in a wavy-walled cavity filled with nanofluid and involving a rotating cylinder, *Entropy*, 20(9), 2018, 664.
[30] Alsabery, A. I., Tayebi, T., Chamkha, A. J., Hashim, I., Effect of rotating solid cylinder on entropy generation and convective heat transfer in a wavy porous cavity heated from below, *International Communications in Heat and Mass Transfer*, 95, 2018, 197-209.
[31] Menni, Y., Azzi, A., Chamkha, A. J., Harmand, S., Analysis of fluid dynamics and heat transfer in a rectangular duck with staggered baffles, *Journal of Applied and Computational Mechanics*, 5(2), 2019, 231-248.
[32] Siddiqui, M. A., Riaz, A., Khan, I., Nisar, K. S., Augmentation of mixed convection heat transfer in a lid-assisted square enclosure utilizing micropolar fluid under magnetic environment: A numerical approach, *Results in Physics*, 18, 2020, 103245.
[33] Bilal, S., Mahmood, R., Majeed, A. H., Khan, I., Nisar, K. S., Finite element method visualization about heat transfer analysis of Newtonian material in triangular cavity with square cylinder, *Journal Materials Research and Technology*, 9(3), 2020, 4904-4918.
[34] Menni, Y., Chamkha, A. J., Azzi, A., Fluid flow and heat transfer over staggered '+' shaped obstacles, *Journal of Applied and Computational Mechanics*, 6(4), 2020, 741-756.
[35] Sheikholeslami, M., Farshad, S. A., Shafee, A., Babazadeh, H., Performance of solar collector with turbulator involving nanomaterial turbulent regime, *Renewable Energy*, 163, 2021, 1222-1237.
[36] Sheikholeslami, M., New computational approach for exergy and entropy analysis of nanofluid under the impact of Lorentz force through a porous media, *Computer Methods in Applied Mechanics and Engineering*, 344, 2019, 319-333.
[37] Sheikholeslami, M., Numerical approach for MHD Al_2O_3-water nanofluid transportation inside a permeable medium using innovative computer method, *Computer Methods in Applied Mechanics and Engineering*, 344, 2019, 306-318.
[38] Bakheet Almatrafi, M., Ragaa Alharbi, A., Tunç, C., Constructions of the soliton solutions to the good Boussinesq equation, *Advances in Difference Equations*, 629, 2020, 1-14.
[39] Nur Alam, Md., Tunç, C., An analytical method for solving exact solutions of the nonlinear Bogoyavlenskii equation and the nonlinear diffusive predator–prey system, *Alexandria Engineering Journal*, 11, 2016, 152–161.
[40] Nur Alam, Md., Tunç, C., New solitary wave structures to the (2+1)-dimensional KD and KP equations with spatio-temporal dispersion, *Journal of King Saud University – Science*, 32, 2020, 3400–3409.
[41] Taylor, C., Hood, P., A numerical solution of the Navier–Stokes equations using finite element technique, *Computers and Fluids*, 1, 1973, 73–100.
[42] Reddy, J. N., *An Introduction to the Finite Element Method*, McGraw-Hill, New York, 1993.

ORCID iD

Md. Fayz-Al-Asad https://orcid.org/0000-0002-1240-4761
Md. Nur Alam https://orcid.org/0000-0001-6815-678X
Cemil Tunç https://orcid.org/0000-0003-2909-8753

How to cite this article: Fayz-Al-Asad Md., Nur Alam Md., Tunç C., Sarker M.M.A. Heat Transport Exploration of Free Convection Flow inside Enclosure Having Vertical Wavy Walls, *J. Appl. Comput. Mech.*, 7(2), 2021, 520–527.
https://doi.org/10.22055/JACM.2020.35381.2646